Liquid-liquid extraction of polyaromatic compounds with ionic liquid. A theoretical and experimental approach

Plácido Arenas-Fernández, Inmaculada Suárez, Baudilio Coto [*]

Chemical, Energy and Mechanical Technology Department, Universidad Rey Juan Carlos, c/Tulipán s/n, 28933 Móstoles (Madrid), Spain

ARTICLE INFO

ABSTRACT

Recent legislation worldwide aims to reduce the levels of polyaromatics compounds in lubricant bases due to their harmful effect on health. Ionic liquids have obtained broad interest as green recyclable extractants. Here, we presented new experimental data of liquid-liquid extraction implementing ionic liquids for the removal of aromatics compounds of synthetic crude oil in a 1:1 mass/mass ratio for temperatures ranging from 303.15 to 293.15 K. Selectivity and distribution constant data are obtained to know the extractive potential of each ionic liquid. To support the experimental results, several computational calculations have been performed. First, two predictive thermodynamic models COSMO-SAC and UNIFAC, have been applied, and the reliability of both models has been compared with experimental results. The results show that using UNIFAC is more accurate than using COSMO to predict extraction behavior. Second, the extractive process has been studied using molecular dynamics. This tool allows us to understand better how the extraction process occurs and the molecules' situation when they reach equilibrium. It is shown that the cation of the ionic liquid is the primary driver of liquid–liquid extraction. In addition, molecular dynamics will enable a qualitative comparison between the performance of ionic liquids and the experimental results. It is a helpful tool to save time and material resources before laboratory experimentation.

1. Introduction

Most lubricant bases originate in crude oil, and their physicochemical characteristics (viscosity, viscosity index, freezing point, volatility…) must meet a series of specifications depending on the final lubricating oil use. The refining process requires reducing aromatic content from these lubricants to upgrade their properties [1–4]. The solvent commonly used is furfural, which has high selectivity toward aromatic compounds [5]. Therefore, a refined product rich in paraffin and an extract rich in aromatic compounds with a large amount of solvent is obtained. This highly aromatic extract is named DAE (Distillate Aromatic Extract) [4,6,7]. Its applications are diverse: formulations of industrial ink, manufacture of cables, and compounds insulation or footwear industry. However, its most widespread use is as an additive in the rubber industry, specifically in manufacturing tires.

On the other hand, some of the PCAs (polycyclic aromatic compounds) included in DAE oils have been classified as carcinogenic, mutagenic, and toxic, proving that they can hurt the health and the environment [8–10]. Due to this and the market growth of this oil, arises

the directive 2005/69/CE of the European Parliament and the Council of November 16, 2005, which, to reduce contamination by PCAs to protect health and the environment, requires that the amount contained in process oils be less than 3 % of its mass from January 1, 2010, onwards. As a reference, the concentration of benzo(a)pyrene is used, with the maximum achievable value being 1 ng/m^3 in an exposure time of one year [11]. For the reasons described above, in recent years, many ways have been studied to reduce the content of these compounds in DAE oils and, therefore, not cause irreversible damage to human health [12]. The most common way to do this is with liquid–liquid extraction, with solvents such as propane, acetone, *n*-hexane, dimethyl ether, and furfural [4,7,13]. That way, DAE oils are transformed in TDAE (Treated Distillate Aromatic Extract). Despite obtaining satisfactory results with the mentioned solvents, using these toxic solvents in large volumes has become a significant concern for health and the environment. That is why alternative solvents have been pursued that meet in terms of efficiency, cost, and toxicity [14].

In recent years, ionic liquids (ILs) have aroused great interest due to their excellent properties and multiple applications in different fields of

chemistry. These compounds are salts in a liquid state below 100 °C, some remaining in this phase even at room temperature, formed by anions and cations of different sizes [15]. They have slight vapor pressure, enabling the likelihood of applying more accessible techniques, such as flash distillation, to recover the ILs from the extract stream [16]. There are a few industrial processes that already use ILs [17] because of their economic benefits and reaction yields, such as the BASIL (Biphasic Acid Scavenging utilizing Ionic Liquids) [18], which employs ILs in the manufacture of alkoxy phenyl phosphines. In this line, several publications have studied the selectivity and extractive capacity of different ionic liquids during the past decade to aromatic compounds [19–22]. It should be noted that the ILs based on the imidazolium and pyridinium cation are the most used in the extraction of aromatic hydrocarbons, proving their viability in treating currents that contain these compounds when their concentration is less than 20 % by weight [23]. Nonetheless, there is undoubted that these products will seep into the environment through production or transportation. Due to their properties, ILs could become permanent pollutants in aquatic systems, so it is essential to evaluate the toxicity effects of ILs on living organisms and the environment [24–26]. The toxicity of Imidazolium and pyridinium based have been studied and could be a threat to marine organisms and microorganisms. In this way, some researchers are now focused on green ILs, such as amino acids-based ILs with less toxicity.

In the vast open literature, some anions implemented in this work, such as $[TF_2N]^-$ and $[BF_4]^-$ are defined as extractors of aromatic hydrocarbons from aliphatic components [15,16,21]; in these studies, the use of these ILs led to high-efficiency aromatics recovery. Moreover, the viscosity is relatively low compared to other ionic liquids, for example, $[EMIm][BF_4]$ (0.06 Pa·s). Indeed, the anion $[TF_2N]^-$ does not decompose to give HF under conditions usually applied for liquid–liquid extractions, as some other typical anions in ILs chemistry do [26]. $[EtSO_4]$ anion is one of the most widely known and cheaper [27,28], so it is always interesting to study its performance.

The solubility of ILs in hydrocarbons is several orders of magnitude lower than that of hydrocarbons in ILs. The solubility of aromatics in ILs is significantly higher than that of aliphatics [16]. This characteristic implies that the selectivity and extraction rates can be higher than those of conventional organic solvents [29].

To identify the ILs with the most significant potential for extracting PCAs, it is necessary to know their thermophysical properties and understand the behavior of the liquid–liquid equilibrium phase during extraction. Due to the many possible combinations that ILs offer, a complete experimental study is not easy. For this reason, developing a model that predicts an IL's extractive capacity based on its molecular characteristics (such as polarity, length of aliphatic chains, or aromaticity) is becoming increasingly necessary.

Different thermodynamic models have been developed to determine the physical and thermodynamic properties of the system [30]; for ILs, classical models such as NRTL [31], UNIQUAC [32], and UNIFAC [33] have been used successfully.

The NRTL (non-random two-liquid model) is a model that correlates the activity coefficients of a compound with its mole fractions in a liquid phase to calculate the phase equilibrium of the mixture. This model is based on Wilson's hypothesis, postulating that the local concentration around a molecule is different from the mass concentration due to the difference in energy of interaction of the central molecule with its exact and another type [34]. The UNIQUAC model is also based on this hypothesis, with the difference that the parameters of this model are relatively insensitive to temperature variation compared to the previous model [35]. UNIFAC is a more predictive model based on the interaction parameters of the groups that make up the molecules [36]. However, although the models in these studies obtain good correlations, much of this information is unavailable, so the analysis using this model is limited to available ions.

The Conductor-like Screening Model for Real Solvents (COSMO-RS) is entirely predictive. COSMO-RS does not need experimental

parameters; thus, it is appropriate to analyze all possible ionic liquids and the extractive power of PCAs [29,37]. This method determines the thermodynamic properties of fluids (for example, the activity coefficient) from quantum mechanics (and helps to know the selectivity and capacity of ILs as solvents [38]. Based on the context of COSMO-RS, Lin and Sandler [39] proposed a modification, the COSMO-SAC (where SAC means ''segment activity coefficient'') model, by invoking a necessary thermodynamic consistency criterion [40]. Even though there are some differences, COSMO-RS and COSMO-SAC share many similarities in the calculation of solvation-free energy and thermodynamic properties. COSMO-SAC model has already been used successfully to screen the ILs used in the extraction process [41,42].

An alternative method to study such systems is molecular dynamics (MD). MD has already been proposed to study ILs [42–44] and is based on the numerical solution of Newton's equation of motion [45]. Different forcefields have been developed to study ILs [43,46–48]. They can obtain experimental values such as shear viscosities, the heat of vaporization, densities, translational self-diffusion coefficients, etc.

This work aims to evaluate the applicability of ILs for this task; we will research PCA's extractive power of 5 ILs. This study will be done theoretically and experimentally in the laboratory using synthetic crude oil (SC). The experimental data will be supported by theoretical data obtained with quantum calculations at COSMO-SAC and by calculations with UNIFAC. UNIFAC model was preferred to other models (NRTL, UNIQUAC) because the number of unknown parameters was much lower, and the comparison to the predictive COSMO-SAC model appears more reasonable. Finally, we will try to relate these results to the data obtained by the MD of the different ILs.

2. Experimental methodology

2.1. Materials

The SC (synthetic crude oil) was prepared with the following weight composition, 64 % of *n*-dodecane ($C_{12}H_{26}$, ≥ 99 %, Sigma Aldrich), 22 % of p-xylene (C_8H_{10}, 99 %, Alfa Aesar), 12 % of 1-methylnaphthalene ($C_{11}H_{10}$, 97 %, Acros organics), and 2 % of pyrene ($C_{16}H_{10}$, 99 %, Acros Organics).

Five ILs were used, 1-ethyl-3-methylimidazolium ethyl sulfate $[EMIm][EtSO_4]$ ($C_8H_{16}N_2O_4S$ > 95 %, Aldrich), 1-ethyl-3-methylimidazolium tetrafluoborate $[EMIm][BF_4]$ ($C_5H_8N_2F_4B$ > 95 %, Alfa Aesar), 1-butyl-3-methylimidazolium tetrafluoroborate $[BMIm][BF_4]$ ($C_7H_{12}N_2F_4B$ > 97 %, Aldrich), 1-butyl-3-methylpyridinium bis(trifluoromethylsulfonyl)imide $[BMPy][TF_2N]$ ($C_{11}H_{20}N_2F_6S_2O_4$ > 97 %, Iolitec) and 1-Hexylpyridinium bromide $[C_6Py][Br]$ ($C_{11}H_{18}BrN$, 99 %, Iolitec).
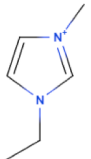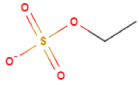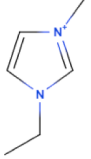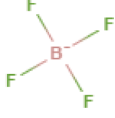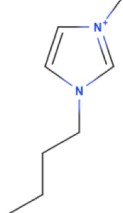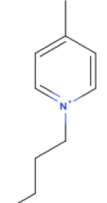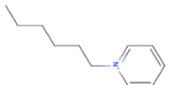
Table 1 lists molecular structures, properties, and characteristics such as decomposition temperature measured by thermogravimetric analysis (TGA) and molecular weight of ILs implemented in this work.

2.2. Liquid-Liquid extraction experiments

To reduce the aromaticity of the SC with the use of ILs, the following experimental steps were done:

– A mixture of SC and IL was put together in a 40 mL vial using 1:1 and 0.5:1 mass ratio IL/SC for each experiment.
– A Teflon-stir at 500 rpm stirred the SC with the IL over an equilibration time of one hour at a specified temperature. The working temperature was controlled using a hot plate.
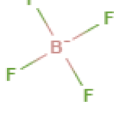– Agitation was turned off, and the vial was kept at constant temperature for another hour until the IL and the organic phase were wholly separated. At this point, the extraction equilibrium is ultimately achieved.
– Higher densities of the ILs make it easier to separate the organic phase. A syringe was used to separate phases to avoid contamination.

Table 1
Properties of ionic liquids employed in this work.

Ionic liquid name	Abbreviation	Cation	Anion	Molar mass (g/mol)	T$_{decomp}$ (°C)[a]	Purity	Supplier	% H$_2$O[b]
1-ethyl-3-methylimidazolium ethyl sulfate	[EMIm][EtSO$_4$]			236.29	393.5	> 95 %	Aldrich	0.05
1-ethyl-3-methylimidazolium tetrafluoroborate	[EMIm][BF$_4$]			197.98	413	> 98 %	Alfa	0.08
1-butyl-3-methylimidazolium tetrafluoroborate	[BMIm][BF$_4$]			226.02	397	≥ 97 %	Aldrich	0.29
1-butyl-3-methylpyridinium bis (trifluoromethylsulfonyl)imide	[BMPy][TF$_2$N]			430.39	429	99 %	Iolitec	0.59
1-Hexylpyridinium bromide	[C$_6$Py][Br]			244.17	405	99 %	Iolitec	0.32

a Decomposition temperature determined by TGA.
b % H$_2$O measured by Karl Fisher Titration.

0.25 mL of each step was transferred to a clean glass vial with 0.7 ml of dichloromethane as solvent.

– Both extract and raffinate phases were analyzed by ^{1}H NMR spectroscopy, according to [2]. ^{1}H NMR determination has been carried out by the assignment of different signals to each component of the sample. Integration of signals has been done by Mestre-Nova software, with an error of about 1 %, and Pyrene is considered as a reference. A linear relationship between relative areas and composition is determined during the calibration procedure, and molar fractions are thus determined.

The liquid–liquid equilibrium and the extraction yield are highly influenced by temperature. The temperatures used in this work were: 30, 50, 70, 80, and 100 °C, less for [C$_6$Py][Br], as it is solid at 30 °C, and their melting point is between 60 and 70 °C; experiments were carried out at temperatures 70, 80, 100, and 120 °C. The IL was preheated at 90 °C for 5 min to guarantee the liquid state. After that was mixed with the SC. In the end, the mixture was cooled down at 70 °C to start the liquid–liquid extraction.

3. Calculation methodology

The systems studied in this work exhibit a splitting phase following a liquid–liquid equilibrium, which is represented by:

$$\gamma_i^r x_i^r = \gamma_i^e x_i^e \tag{1}$$

where γ_i and x_i are the activity coefficient and mole fraction of

component i, superscripts SC-r and IL-e refer to the organic and ionic liquid phases, respectively.

Considering the advantages and disadvantages of the models explained in the introduction, this paper considers two thermodynamic models, COSMO-SAC and UNIFAC, for activity coefficient determination.

3.1. COSMO-SAC model

In this work, the COSMO-SAC model was used to determine liquid–liquid equilibrium. To begin with, quantum mechanical calculation and geometry optimization of ILs were carried out using Turbomole. COSMO-RS model describes interaction energies between molecules which are calculated from electronic densities computed through the density functional theory (DFT).

The IL is introduced as a pseudo component with specifications for average boiling temperature, molar mass, and density requested as specific gravity in the simulation process. In addition, it is necessary to include the vapor pressure since it is one of the characteristic properties of this type of compound. A value of -1×10^8 is introduced for the Antoine coefficient in the first data of the PLXANT parameter [49] to represent that the mixture is not volatile. The rest of the compounds are introduced as conventional compounds. Moreover, for each component, it is necessary to specify the molar volume parameter in cubic Armstrong (CSACVL) and the sigma profile (σ-profile). In the COSMO-SAC model, molecular interactions are calculated from the interactions between the surface charge distributions of the molecules in contact. There are three

ways of treating ILs, collected by Lee and Lin [50], and each one leads to differences in the calculation of properties and equilibrium:

1. Ion model: they are treated as two individual ionic species in the COSMO calculation model and the COSMO-SAC model.
2. C + A model: they are treated as individual species for the calculation, but the σ profiles are combined in the COSMO-SAC calculation as an IL ion pair (*meta*-file model).
3. Molecule model: they are treated as neutral molecules in the COSMO and COSMO-SAC calculations.

C + A model is the method employed in this work due to being quite successful and was found to be superior to the molecule model for ILs in mixture systems, as in our case [50,51]. Sigma-profile data used for COSMO-SAC simulation are found in Fig. 3 of the supplementary material.

3.2. UNIFAC model

UNIFAC is a predictive thermodynamic model used to calculate nonelectrolyte activity in nonideal mixtures. This model is based on experimental information, and interaction parameters of the IL could be treated as a group contribution method or the cation and anion as independent molecules.

According to the UNIFAC model [52], activity coefficient γ_i of i component in the liquid phase is calculated by:

$$\ln(\gamma_i) = \ln(\gamma_i)^C + \ln(\gamma_i)^R \tag{2}$$

The combinatorial part includes the volume of the component i and its surface fraction while the residual part is obtained from the activity coefficient of each group. The group interaction parameter is also needed and is defined by Eq. (3):

$$\Psi_{nm} = exp\left(-\frac{a_{nm}}{T}\right) \tag{3}$$

where a_{nm} are UNIFAC group binary interaction parameters between groups n and m, all data needed for the simulation (Van der Waals volumes, molecular surface areas, and binary interaction parameters) were obtained from Lei [36,52].

The interaction parameter of [C$_6$Py][Br] was not available and was determined in this work. Structural R_k and Q_k values for the [Py][Br] group were determined by group addition from values for Pyridine and Br groups. Interaction parameters were obtained by minimizing the standard deviation between experimental mole fractions and those calculated by the UNIFAC model. Therefore, for the UNIFAC model, there is the possibility of changing the interaction parameters so that the model is as close as possible to the experimental results. The bibliographic parameters used [36,52] shown in Table 2 were obtained for binary aliphatic/monoaromatic mixtures without the presence of polyaromatic compounds, so the parameters that are modified are those corresponding to the interactions of IL with the aromatic rings and vice versa (for example PYBTI-AC, PYBTI -ACH, AC-PYBTI, and ACH-PYBTI). These values are modified individually, and in the sense that the relative

deviation of the compositions is minimized, according to Eq. (4). The [-Py][Br] group values were determined from the experimental data.

$$\%DRAT = \frac{100}{n-1} \cdot \sum_{i=1}^{n} \frac{\left|x^j_{i,exp} - x^j_{i,UNIFAC}\right|}{x^j_{i,exp}} \tag{4}$$

where $x^j_{i,exp}$ is the experimental value of the composition, and $x^j_{i,UNIFAC}$ is the value calculated by the simulation using the UNIFAC model. Most group parameters R_k and Q_k presented in Table 3 were also found in the bibliography [36,52], and estimated in this work for group [-Py][Br].

3.3. Molecular dynamics simulation

The present work studied IL-SC equilibrium by computing MD using GROMACS 4.5.3 molecular dynamics package [53]. To begin with, SC and ILs molecules were painted using Avogadro Software. After that, topology prediction was obtained by making use of the CGENFF program. CHARMM General Force Field has shown to be the more reliable choice than other forces field fields OPLS-AA or Amber for studying ILs [54–57]. CHARMM general energy function is shown in Eq. (5):

$$E = \sum_{Bonds} K_b(b - b_0)^2 + \sum_{angles} K_\theta(\theta - \theta_0)^2 + \sum_{U-B} K_{UB}(u - u_0)^2 + \sum_{dihedrals} K_\Phi[1$$

$$+ (n\emptyset - \delta)] + \sum_{improper} K_w(w - w_0)^2 + \sum_{nonbonded} \left\{ \varepsilon_{ij}\left[\left(\frac{R_{min,ij}}{r_{ij}}\right)^{12}\right.\right.$$

$$\left.\left. + \left(\frac{R_{min,ij}}{r_{ij}}\right)^6\right] + \frac{q_i q_j}{4\pi D r_{ij}}\right\}$$

$$\tag{5}$$

where K_b are the bond forces and $b - b_0$ the distance from initial equilibrium which each atom has moved forward; K_θ are the angle forces and $\theta - \theta_0$ is the equilibrium angle; At the third term of Eq. (5) Urey-Bradley potential and distance are defined by K_{UB} and $u - u_0$; At the fourth term of Eq. (5) K_Φ shows the dihedral forces constant while n is the multiplicity function, $\emptyset$ the dihedral's angle and δ is the phase shift; next, K_w is the improper force constant and $w - w_0$ the improper angle; Last term of the Eq. (5) shows Lennard-Jones potentials useful to predict van der Waal's forces and Coulomb's potential. Finally, $R_{min,ij}$ q and D denote the distance at the Lennard-Jones minimum potential between atoms, the atomic charges, and the dielectric constant, respectively [58]. Once the forcefield was optimized for each compound, MD simulation conditions were stablished. At the beginning, a box containing only the SC was simulated. This box had a size of 5 nm × 5 nm × 5 nm, and to maintain the weight ratio of the experimental SC, the box contained 4 molecules

Table 3
Group Parameters of Volume R_K and Surface Area Q_k.

Parameter	[–Py][TF$_2$N]	[-MIm][BF$_4$]	[-MIm][-SO$_4$]	[-Py][Br]
R	5.8237	6.5669	9.2723	3.9486 [a]
Q	4.7313	4.005	6.3238	2.945 [a]

[a] Values calculated in this work.

Table 2
Bibliographical and experimental group interaction parameters for the UNIFAC model.

	Group j	Group j	Group j	Group j	Group j	Group j	Group j
Group i	CH2	ACH	ACCH2	(M)PYBTI	[-MIm][BF$_4$]	[-MIm][-SO$_4$]	[-Py][Br]
CH2	–	61.13	76.5	327.3	1108.51	384.22	1500 [a]
ACH	−11.12	–	167	998.04	1494.39	1165.01	1200 [a]
ACCH2	−69.7	−146.8	–	−139.79	55.96	−117.73	1400 [a]
[-Py][TF$_2$N]	301.96	−131.54	644.47	–	–	–	–
[-MIm][BF4]	588.74	85.64	1834.88	–	–	–	–
[-MIm][-SO$_4$]	394.94	28.01	881.53	–	–	–	–
[-Py][Br]	120 [a]	180 [a]	220 [a]	–	–	–	–

[a] Values calculated in this work.

of pyrene, 84 of p-xylene, 32 of 1-methylnaphthalene and 300 of *n*-hexane which was used instead of *n*-dodecane with the aim to decrease the number of degrees of freedom, speeding up the simulation. This decision is supported by other studies where it was shown that there is no great difference between hexane and dodecane in MD as they both are apolar and have a long chain [57]. The initial configuration of the SC box was minimized using the steepest decent method for 10.000 ps. The constant volume temperature ensemble (NVT) equilibration was realized at three different temperatures (30, 50, and 70 °C). Next, the box was equilibrated in the constant pressure-constant temperature ensemble (NPT) making use of Langevin dynamics with a time step of 0.1 fs, the total duration was 10.000 ps setting pressure at 1 atm. Temperature was kept constant using the Nosé – Hoover [59] algorithm while pressure was keep constant with Parinello − Rahman algorithm [60]. Finally, a MD simulation was performed for the duration of 5 ns for the SC box. This procedure was also applied for each IL, where a box with a size of 5 nm × 5 nm × 5 nm was created and filled with IL molecules. The validation of the MD simulation was done studying the density of the solutions. The density of some ILs at 30, 50 and 70 °C was found through the databank ilthermo.boulder.nist.gov, otherwise Anton Paar SVM 3000 was put into use to obtain it (SC density was also validated). This density was compared to that obtained by MD which can be found in Fig. 1 of the supplementary material. As can be seen the error obtained was under 2.5 % which is a good approximation. At the end, SC and IL boxes were joined creating a box of 5 nm × 10 nm × 5 nm in size as can be seen in Fig. 1. Following, another NPT equilibration was done with the aim to equilibrate the two layers in contact. After all, MD simulation was run for the duration of 20 ns. This time-scale simulation has been shown in previous studies to be appropriate and to achieve high efficiency [57,61].

4. Results and analysis

4.1. Experimental results

As previously commented, liquid–liquid extractions are carried out between the IL and the SC. Once equilibrium was reached, the top and bottom layers were analyzed by ^{1}H NMR spectroscopy. The experimental compositions for the liquid–liquid equilibrium phases are placed in Table 4, which lists temperature values for each IL and the mole fraction for the five compounds in the extraction in both the raffinate and extract phases. All the experiments were performed at atmospheric pressure. Fig. 2 of the supplementary material shows a typical [1]H-NRM of the SC and the IL [BMPy][TF₂N]. The analyzes show that the separation between the ILs and the synthetic crude is greater than 99 % since no trace of IL is found in the NMR of the upper layer. In addition, the amount of dodecane in the IL phase (down layer) was also negligible, as seen in Table 4. The systematic error of the ^{1}H NMR results is 1 % of its
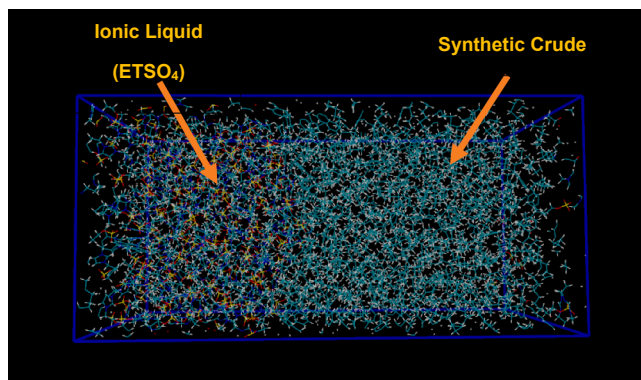
absolute value.

The experiments were done with temperatures ranging from 30 to 120 °C; Fig. 2 shows the extraction data for methylnaphthalene and p-xylene for each temperature. We can see that methyl naphthalene is extracted a little more in percentage than p-xylene. This may be due to several factors; on the one hand, two aromatic rings in the methyl naphthalene may influence a more significant interaction between these molecules and the ionic liquid. On the other hand, p-xylene is completely nonpolar, which can decrease the ionic liquid's extractive force. Nonetheless, the proportion of methyl naphthalene in the SC is only 12 % by weight, while that of p-xylene is 22 %. Therefore, obtaining a lower total percentage extracted is logical because as the net amount increases, it becomes more challenging to reduce the total rate. Through MD, the interaction of both molecules with the IL will be analyzed a little better. If we observe the extractive capacity of each ionic liquid, in both cases, [BMPy][TF₂N] presents a higher yield; the only exception is [C₆Py][Br] at 120 °C for p-xylene. However, the variation with the rest of the ILs is not too significant (around 10 % in performance). Several studies have already shown the cation [BMIm] to have a higher extractive capacity than the cation [EMIm] [57,62], especially with aromatics compounds, here [BMIm][BF₄] has about the same capacity as the [C₆Py][Br] and is slightly better than the [EMIm][BF₄]. The larger aliphatic butyl chain infers a higher polarity to the molecule and a higher yield. Finally, the [EMIm][BF₄] and the [EMIm][EtSO₄] are the ones with the worst qualities, having a 15 % lower performance than the [BMPy][TF₂N]. Regarding temperature, the extraction values are not highly affected by it. For methyl naphthalene, they have a slightly decreasing trend but less than 5 %; for p-xylene, they mostly have an upward trend, but it is also not very significant. As we will see in the simulation section, the temperature does affect the mole fraction of each phase a little, but to a lesser extent, the total percentage of aromatics extracted.

Fig. 3 shows the extractive capacity of pyrene. As we can see, the extractive power of IL is much lower in a polyaromatic compound such as pyrene than in diaromatic or monoaromatic compounds such as methylnaphthalene and p-xylene. Although the percentage of pyrene in the SC is low, only the [BMPy][TF₂N] manages to exceed 50 % extraction. This makes sense because of its low polarity and structure, making it stable in *n*-dodecane. The extractions are carried out thanks to the π-π interactions between the pyrene rings and the ILs rings.

[BMPy][TF₂N] is the one that has better performance extracting polyaromatics compounds. Previously in other works, anion [TF₂N] was an excellent solvent for liquid–liquid extraction processes for separating aromatic and polyaromatic compounds [16,49]. After [BMPy][TF₂N], it is the [C₆Py][Br] one that shows better behavior, a little descending with the temperature. Next is the [BMIm][BF₄], whose performance also drops a little with temperature, and at 100°, it is practically the same as that of the [EMIm][EtSO₄], whose performance is barely affected at different temperatures. Finally, we find [EMIm][BF₄] as the ionic liquid with the worst performance in general. We can conclude that between [BMIm] and [EMIm] cations in [BMIm], the one who works better, and between [BF₄] and the [EtSO₄] anions, [EtSO₄] works better. The IL [BMIm][EtSO₄] should be synthesized and tested since it will predictably give a higher yield.

We wanted to see how the mass/mass ratio influences the extraction yield. For the [EMIm][EtSO₄] and [BMPy][TF₂N] ILs, in addition to a 1:1 IL/SC ratio, a 1:2 ratio was also made. As seen in Fig. 4, the extractive yield drops around 30 percent when the amount of IL decreases by half. This information will be useful in optimizing the required amounts of IL in the feed when scaling up the process.

The feasibility of using the IL as polyaromatic extractor is evaluated by distribution constant (K_i) and selectivity (α_i) given by next equations:

Fig. 1. Initial simulation conditions. The two layers formed by the ionic liquid and the synthetic crude are in contact.

$$K_i = \frac{x_i^e}{x_i^r} \tag{6}$$

Table 4

Experimental LLE data in mole fractions for each IL at different temperatures and atmospheric pressure. The system components are *n*-dodecane(1), methylnaphthalene(2), p-xylene(3), pyrene(4) and IL(5).

|	T (°C)	Extract					Raffinate				
		x_1	x_2	x_3	x_4	x_5	x_1	x_2	x_3	x_4	x_5
[EMIm][EtSO$_4$]	30	0.0619	0.0394	0.0401	0.0118	0.8468	0.8217	0.0471	0.1179	0.0114	–
	50	0.0117	0.0331	0.0314	0.0109	0.9129	0.8167	0.0476	0.1223	0.0115	–
	70	0.013	0.0345	0.0339	0.011	0.9077	0.8203	0.0474	0.1187	0.0117	–
	80	0.0109	0.024	0.0222	0.01	0.946	0.8295	0.0418	0.1172	0.0116	–
	100	0.0089	0.0278	0.0262	0.0091	0.9279	0.8252	0.0463	0.1152	0.0114	–
[EMIm][BF$_4$]	30	0.0192	0.0228	0.0245	0.0065	0.927	0.8136	0.0492	0.1224	0.013	–
	50	0.0103	0.0221	0.0227	0.0064	0.9385	0.8152	0.0491	0.1209	0.0129	–
	80	0.0059	0.0227	0.0255	0.007	0.939	0.8185	0.0495	0.1171	0.013	–
	100	0.0058	0.0216	0.0235	0.0068	0.9423	0.8203	0.0498	0.1151	0.0129	–
[BMIm][BF$_4$]	30	0.0245	0.0334	0.0389	0.0101	0.8931	0.8306	0.0422	0.1149	0.0104	–
	50	0.0426	0.0366	0.0431	0.0107	0.8669	0.8285	0.0441	0.1146	0.011	–
	80	0.0136	0.037	0.0425	0.0107	0.8963	0.8317	0.0437	0.1118	0.0109	–
	100	0.0117	0.0343	0.0393	0.0079	0.9068	0.8305	0.0452	0.1111	0.0113	–
[BMPy][TF$_2$N]	30	0.0275	0.0922	0.0889	0.0051	0.7863	0.8636	0.0289	0.0991	0.0066	–
	50	0.0275	0.0999	0.0791	0.0167	0.7768	0.8645	0.0295	0.0974	0.0067	–
	80	0.0255	0.0706	0.0675	0.0167	0.8198	0.8608	0.0321	0.0977	0.0075	–
	100	0.0311	0.0681	0.0667	0.0163	0.8178	0.8656	0.029	0.0977	0.006	–
[C$_6$Py][Br]	70	0.019	0.0298	0.0346	0.0086	0.9251	0.8293	0.0439	0.115	0.0099	–
	80	0.019	0.0299	0.0278	0.0093	0.9312	0.8363	0.0424	0.1098	0.0097	–
	100	0.0177	0.0313	0.031	0.0093	0.9266	0.8368	0.043	0.1083	0.01	–
	120	0.0256	0.0267	0.0257	0.0085	0.9373	0.8722	0.0446	0.0711	0.0103	–
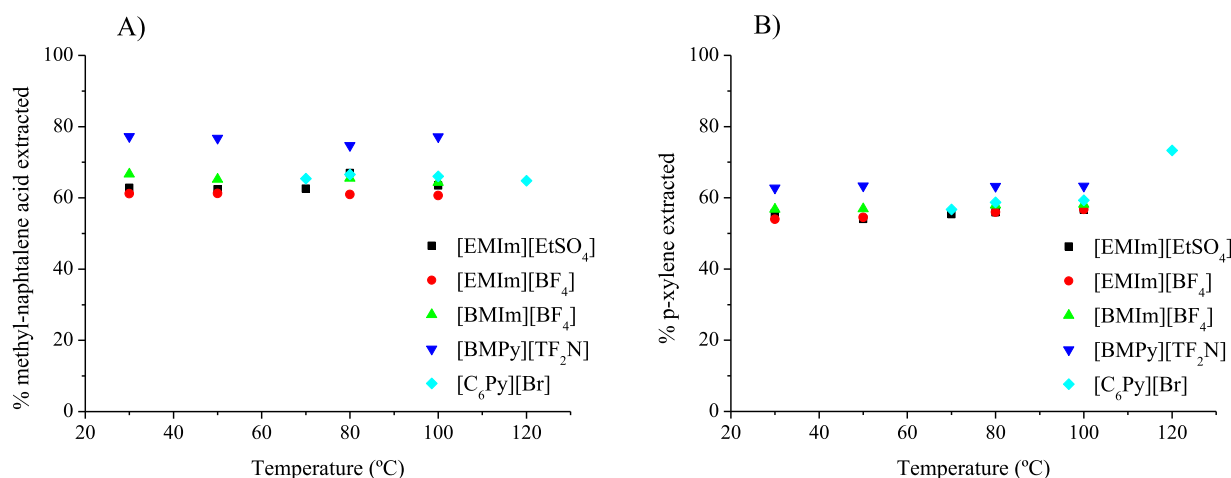
Fig. 2. A) Percentage of extraction of methyl naphthalene for each ionic liquid at different temperatures B) Percentage of extraction of p-xylene for each ionic liquid at different temperatures.

$$\alpha_i = \frac{K_i}{K_D} \qquad (7)$$

where subscript i refers to each of the components of the synthetic crude, x_i^e is the mole fraction of each compound in the extract, and x_i^r is the mole fraction of each compound in the raffinate. K_D is the distribution constant of the aliphatic compound (*n*-dodecane) and is used as reference to calculate de selectivity of the aromatic compound.

To study the solvent's quality, the current values of α and K must be analyzed. Fig. 5 A plots values of α vs K for methylnaphthalene in each IL. Fig. 5 B and C do the same for p-xylene and pyrene. α values for the three compounds are prevalent, ranging between 10 and 110 for methylnaphthalene, (5–30) for p-xylene, and (13–78) for pyrene. In the same way, for the K values, methylnaphthalene presents the most extensive range (0.4–3.2), p-xylene the smallest (0.2–0.9), followed by pyrene (0.5–2.7); therefore, higher extraction efficiencies are expected for methylnaphthalene as it was shown in Fig. 2 A).

Among all the ILs, the one that has presented higher values of α and K is the [BMPy][TF$_2$N]. Thus [BMPy][TF$_2$N] has good properties as a solvent for liquid–liquid extraction processes for separating aromatic and polyaromatic compounds. The solute distribution ratio and selectivity values are good enough, being better than those for furfural, which is the standard common reference for these purposes [2,13]. Among the rest of the ILs is as expected [EMIm][BF$_4$], the one with the lowest distribution constant. [BMIm][BF$_4$], [EMIm][EtSO$_4$] and [C$_6$Py][Br] have analogous results, thus a similar behavior in them is expected.

4.2. Thermodynamic model results

A comparison was made between the results obtained by a predictive method such as COSMO-SAC and those obtained by UNIFAC. As mentioned above, carrying out a prior validation stage is necessary. After the simulation, an extract and a raffinate are obtained, whose results in the mole fraction are compared with those obtained experimentally. These data present a particular deviation, as reflected in Table 1 of the supplementary material, getting better outcomes for the UNIFAC model.

In Table 1 of the supplementary material, we can find all the experimental and computational results for a temperature of 80 °C in each IL. It compares the mole fractions of each component of the SC both
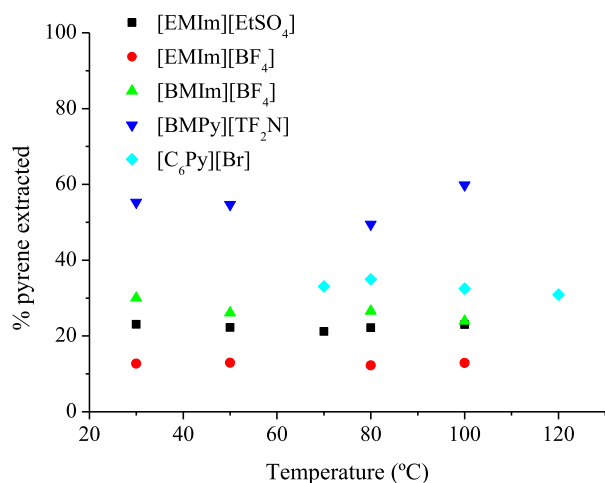
Fig. 3. Percentage of extraction of pyrene for each ionic liquid at different temperatures.
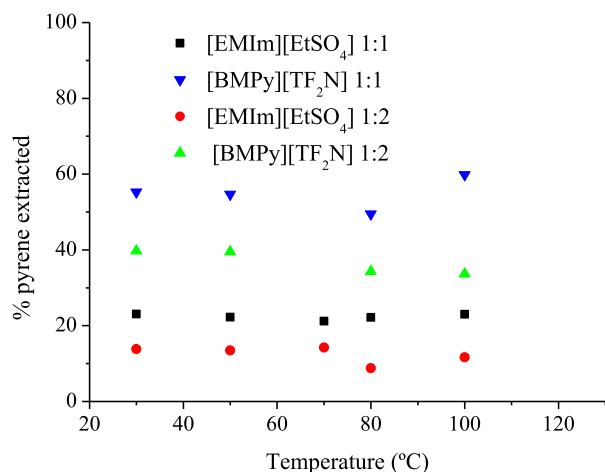

Fig. 4. Percentage of extraction of pyrene for [EMIm][EtSO$_4$] and [BMPy] [TF$_2$N] in a mass/mass IL/SC ratio of 1:1 and 1:2.

in the extract and the raffinate. A comparison can be made between the results obtained in the refining experimentally and those obtained in the refining using UNIFAC and COSMO-SAC. If we take a close look, It can be seen, as expected, that UNIFAC results are much more similar to the experimental ones than those obtained by COSMO-SAC. The data obtained with COSMO-SAC have an average of 18 % more error. As other authors refer to in their works [13,40], COSMO-SAC should be taken as a

good starting point but must still be improved, and it should always be compared with the experimental data.

This previously detailed comparison can be seen more visually in Fig. 6, where the selectivity of the different compounds is represented against the distribution constant for [EMIm][BF$_4$] and [BMIm][BF$_4$] obtained both experimentally and computationally. It can be seen how the data obtained at UNIFAC (green) are much more like the experimental data (black) than the data obtained by COSMO-SAC. The data for methylnaphthalene in COSMO-SAC does not appear in both graphs because the selectivity was too high (around 1000) and made the display of the chart worse. The selectivity prescribed by COSMO-SAC is oversized and too large. Another comparison that can be made is how the distribution constants of methyl naphthalene and pyrene are slightly higher than those of p-xylene, being higher than that of pyrene. Their selectivity is also quite similar, but there seems to be a tendency where ILs more easily extract compounds with higher aromaticity. The distribution constant of ILs represented in Fig. 6 is ordered from largest to smallest pyrene > methylnaphthalene > p-xylene according to greater aromaticity to a smaller one. For the rest of the ILs, depending on the IL used, the distribution constant will be greater for pyrene for m-naphthalene, and in all cases, for p-xylene, it will be the smallest.

4.3. Molecular dynamics results

GROMACS software was used to study the behavior of ILs in contact with SC oil. Simulations were developed with a time scale long enough to reach phase equilibrium. The MD simulation will consist of a qualitative analysis showing each IL's tendencies to extract polyaromatic components. As previously commented, MD simulations were performed with a time-scale of 20 ns at 30, 50, and 70 °C. The proportions of IL and SC used have been the same used experimentally, 1:1 mass ratio. To do this, the number of molecules of each compound has been calculated.

As shown in Fig. 1, the IL and the SC were separated at the beginning of the simulation, forming two different phases. At the endpoint of the experiment, it was possible to observe how the aromatic components present in the SC had diffused into the phase formed by the IL until phase equilibrium was reached. This can be seen in Fig. 7, where we have a snapshot of the [C$_6$Py][Br] simulation endpoint. All SC components except methylnaphthalene have been deleted from the image. It can be seen how this diaromatic compound has largely diffused into the phase formed by the ionic liquid. Another small percentage has remained in the stage that includes the SC, which is the gap that is observed to be empty.

In the same way, this observation has been made for the rest of the SC components, where it has been seen that *n*-hexane does not diffuse towards IL in any case, as happens with *n*-dodecane experimentally. Fig. 8 shows the simulation endpoint of the [EMIm][BF$_4$], where only the IL and the pyrene molecule are shown. 3 of the four pyrene molecules were
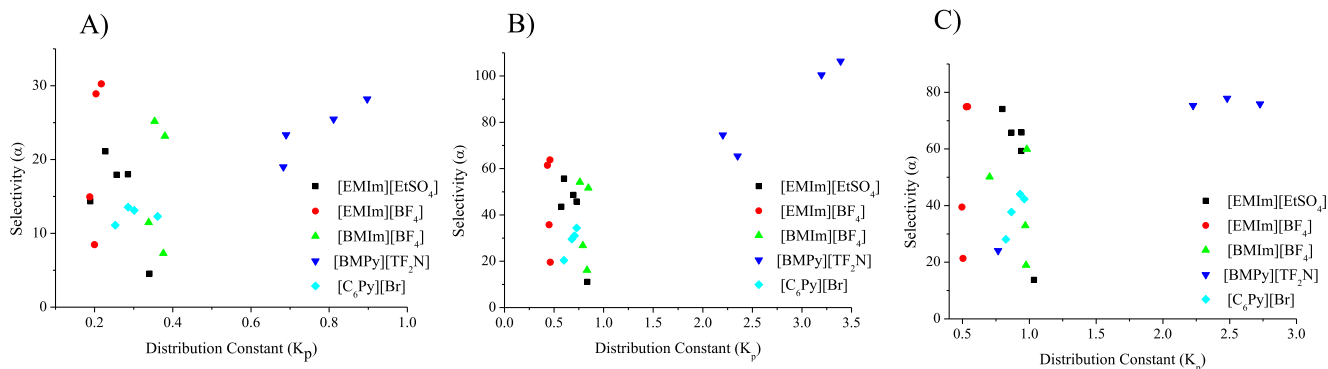

Fig. 5. A) Selectivity for methylnaphthalene vs distribution constant in each ionic liquid. B) Selectivity for p-xylene vs distribution constant in each ionic liquid. C) Selectivity for pyrene vs distribution constant in each ionic liquid.
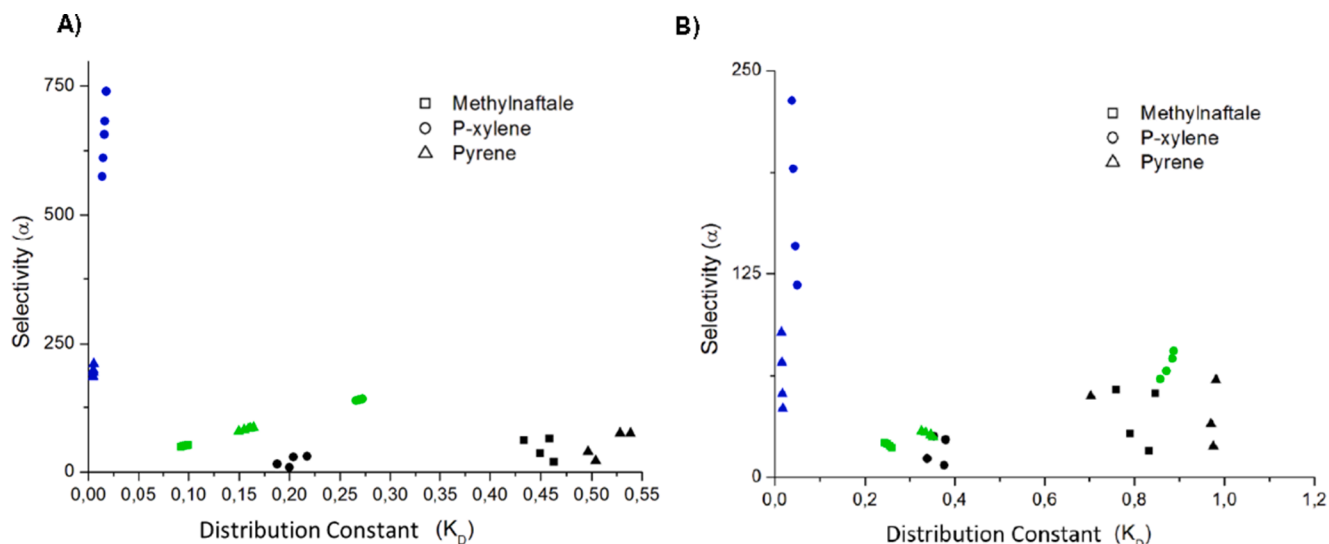
Fig. 6. Comparison of selectivity versus distribution coefficient of experimentally obtained data (black), COSMO-SAC data (blue), and UNIFAC data (green). A) For the [EMIm][BF₄] ionic liquid. B) For the the [BMIm][BF₄] ionic liquid. (For interpretation of the references to colour in this figure legend, the reader is referred to the web version of this article.)
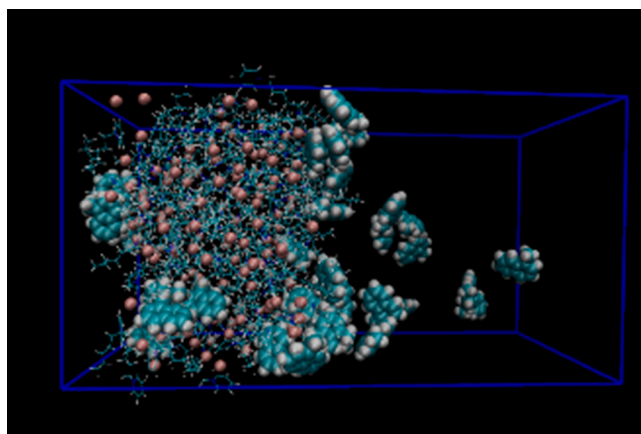

Fig. 7. Final result of the molecular dynamics simulation. Phase equilibrium in the extraction of methylnaphthalene using [C₆Py][Br].

extracted by the IL after the simulation. But another appreciation of this molecule is its difficulty diffusing inside the IL, mainly staying on its surface phase. This is due to the larger size and lower diffusion coefficient than p-xylene and methylnaphthalene. For this reason, in poly-aromatic extraction phenomena, the extraction surface can play a crucial role in achieving phase equilibrium. Another factor affecting the diffusion of aromatics can be the surface tension and the diffusion coefficient of ILs. In general, the higher its diffusion coefficient was, the greater the diffusion of polyaromatics within the IL.

Another analysis that can be done is the percentage of aromatics that extract the ILs. Table 5 shows the percentage of methylnaphthalene, p-xylene, and pyrene that every-one of the ILs has extracted on average at each temperature. These results have been obtained thanks to the GROMACS clustsize tool. MD error data were obtained using the radial distribution function. With this, it has been possible to obtain the number of polyaromatic molecules on average in each phase, and with this data, the total percentage extracted has been calculated. It can be seen how [BMPy][TF₂N] is the IL that, on average, extracts the highest percentage of aromatics, followed by [C₆Py][Br]. [EMIm][BF₄] and
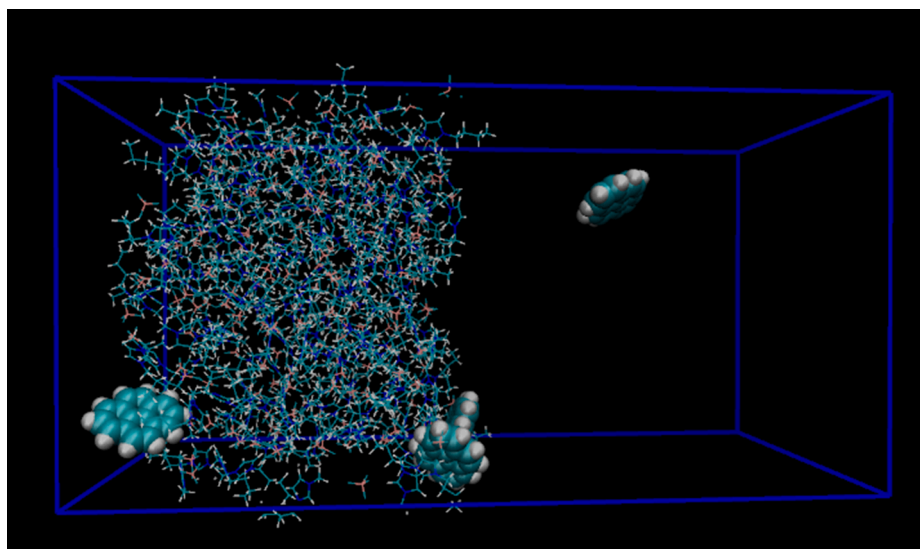

Fig. 8. Simulation endpoint snapshot. Phase equilibrium for pyrene, in the extraction with [EMIm][BF₄].

Table 5
Percentage of extraction of Methylnaphthalene, P-xylene, and Pyrene at three different temperatures with each ionic liquid. The average aggregation throughout the molecular dynamics simulation results is obtained.

	Metylnafthalene			P-xylene			Pyrene		
	303.15 K	323.15 K	343.15 K	303.15 K	323.15 K	343.15 K	303.15 K	323.15 K	343.15 K
[EMIm][EtSO$_4$]	54.69 ($\pm$1.42)	56.44 ($\pm$1.75)	45.53 ($\pm$1.23)	72.02 ($\pm$1.88)	69.00 ($\pm$2.14)	57.17 ($\pm$1.55)	58.25 ($\pm$1.52)	50.08 ($\pm$1.55)	47.75 ($\pm$1.29)
[EMIm][BF$_4$]	63.16 ($\pm$2.05)	44.53 ($\pm$1.44)	44.84 ($\pm$1.45)	70.15 ($\pm$2.28)	58.31 ($\pm$1.89)	56.71 ($\pm$1.84)	64.50 ($\pm$2.10)	41.50 ($\pm$1.35)	52.75 ($\pm$1.71)
[BMIm][BF$_4$]	64.16 ($\pm$1.96)	48.69 ($\pm$1.48)	48.41 ($\pm$1.48)	73.44 ($\pm$2.24)	60.65 ($\pm$1.85)	57.39 ($\pm$1.75)	79.75 ($\pm$2.43)	60.50 ($\pm$1.85)	64.25 ($\pm$1.96)
[BMPy][TF$_2$N]	70.69 ($\pm$2.91)	62.38 ($\pm$2.57)	60.44 ($\pm$2.49)	78.73 ($\pm$3.24)	74.10 ($\pm$3.05)	71.98 ($\pm$2.96)	89.00 ($\pm$3.66)	75.50 ($\pm$3.11)	76.50 ($\pm$3.15)
[C$_6$Py][Br]	67.22 ($\pm$2.58)	52.81 ($\pm$2.03)	54.69 ($\pm$2.10)	75.21 ($\pm$2.89)	69.39 ($\pm$2.66)	65.83 ($\pm$2.53)	74.25 ($\pm$2.85)	69.00 ($\pm$2.65)	57.75 ($\pm$2.22)

[EMIm][EtSO$_4$] are the two worst performers. A qualitative comparison can be made with experimental results where that order of action was obtained. These extraction percentages are slightly higher than those obtained experimentally, but the objective of DM is not to achieve net results. The MD is a useful tool to predict the behavior of every-one of the ILs and save laboratory experimentation, but never as a substitute for the experimental results.

Analyzing the effect of temperature on extraction, the percentage of aromatics extracted generally decreases as temperature increases. Experimentally, it was observed that the ILs decreased their extraction very slightly with temperature, except for [C$_6$Py][Br], where the efficiency increased in the range of temperatures studied. Here the decrease is much more pronounced, and particles are more affected by the temperature change.

One of the primary purposes of studying extraction processes by MD is to understand how this extraction mechanism occurs [57]. In Fig. 9, you can see the radial distribution function of [BMIm][BF$_4$] concerning A) methylnaphthalene, B) p-xylene, and C) pyrene. Black lines show that the radial distribution respect the cation, and red lines respect the anion. In all cases, red lines present a peak before black lines, indicating a greater probability of finding the cation and then the anion. This is of vital importance when it comes to understanding the extraction process of aromatics. Since our ILs have cyclic aromatic structures, it makes sense to find first the cation and then the anion. The extraction process of aromatics could occur through π-π interaction between aromatic rings. In the same way as [C$_6$Py][Br] and [BMPy][TF$_2$N], its cycle presents three double bonds, while [EMIm] and [BMIm] have only two; this π-π interaction will occur more strongly in [C$_6$Py][Br] and [BMPy][TF$_2$N], therefore it agrees with higher performance in the experimental extraction process. Thus, it also makes sense that selectivity progressively improves from p-xylene to methylnaphthalene as aromaticity increases. The cation is believed to be the primary driver of this

extraction process and will affect its structure more than the anion.

Finally, the diffusion coefficients of the different ionic liquids have been studied employing the Einstein-Helfand approach. Looking at bibliographic data, slight variations in the diffusion let coefficients calculated by MD simulations are observed, ranging from 0.1x10^{-12} to 100x10^{-12} m^2/s [48,63–66]. This range is within the data obtained in this work, which can be seen in Fig. 10. It exhibits the variation of cations and anions' diffusion coefficient as a temperature function. As in the experimental results, the diffusion coefficient is slightly higher for the cation than for the anion. This is due to cations' greater size and polarizing power from used molecules. When diffusion coefficients are compared with the data obtained in Table 5, those ILs which present a greater extraction of aromatics are those ILs that have a lower diffusion coefficient, being [EMIm][EtSO$_4$] and [EMIm][BF$_4$], the two that have the most excellent diffusion and the worst performance. Still, this correlation cannot be made general since dynamic properties are compared with equilibrium properties. As temperature increases, the diffusion coefficient rises, and interestingly, the IL extraction capacity decreases, as shown in Table 5. Higher temperatures allow higher diffusion coefficients and let molecules come into greater contact. As temperature increases, de diffusion coefficient and selectivity decrease reducing liquid–liquid separation. The equilibrium constant is shifted to the left, and less extraction will generally occur as the temperature increases. We are working with SC, whose viscosity is relatively low; in real base oils, the thickness can be a crucial factor in the equilibrium constant. Therefore, it is expected that the maximum extraction in factual bases will be at slightly higher temperatures with a lower viscosity.

5. Conclusions

Removing polyaromatics compounds from lubricant bases is a typical arduous separation process. The most used solvent is furfural, but
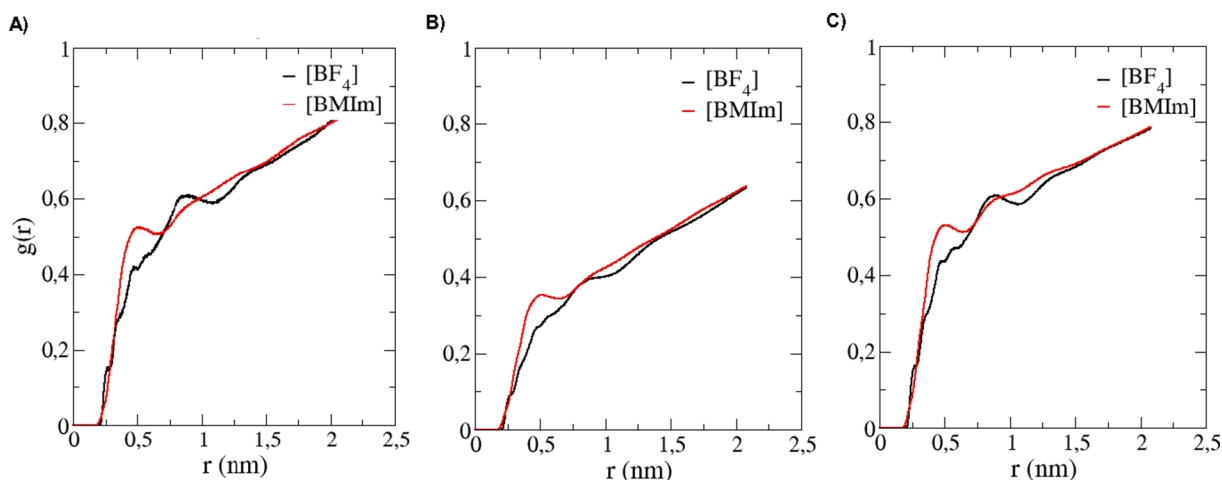

Fig. 9. A) Radial distribution function of methylnaphthalene respect [BMIm][BF$_4$]. B) Radial distribution function of p-xylene respect [BMIm][BF$_4$]. C) Radial distribution function of pyrene respect [BMIm][BF$_4$]. In all cases, a distinction is made between the cation [BMIm] (red) and the anion [BF$_4$] (black). (For interpretation of the references to colour in this figure legend, the reader is referred to the web version of this article.)
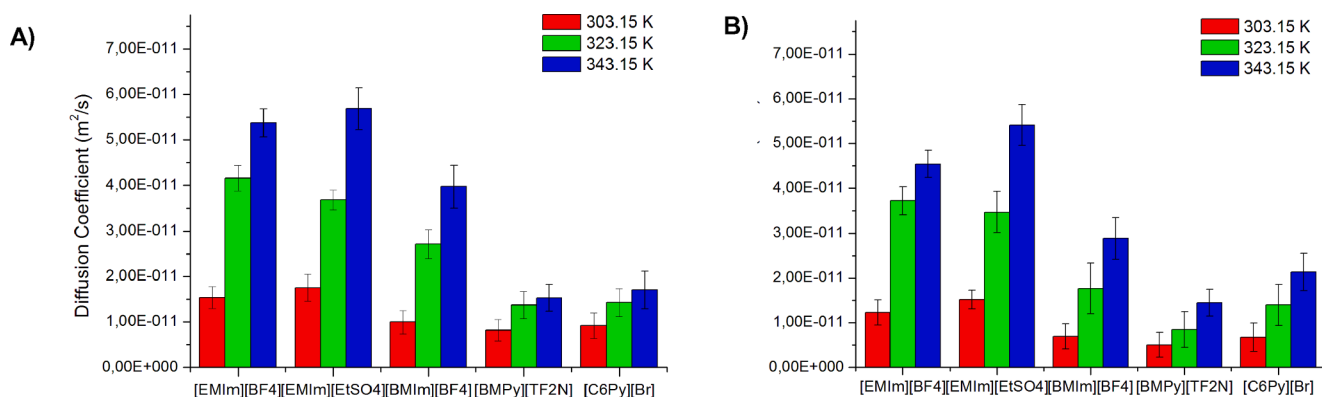
Fig. 10. A) Diffusion coefficient of the cation of each ionic liquid at three different temperatures. B) Diffusion coefficient of the anion of each ionic liquid at three different temperatures.

it has been shown that ILs have the potential to remove aromatic compounds with high performance. Of the different ILs used, the one with the highest yield is [BMPy][TF$_2$N]. This higher yield has subsequently been related to its aromaticity. In the range of temperatures studied, the extraction performance is slightly affected. It seems that most ILs have a slight tendency to decrease their extraction efficiency as temperature increases, except for [C$_6$Py][Br], which has increased. If we halve the amount of IL used by mass, the yield drops by around 30 %.

The experimental results obtained have been compared with computational results, where two different thermodynamic models, UNIFAC and COSMO-SAC, have been used. Analyzing the data shows how UNIFAC predictions are more accurate than those of COSMO-SAC. Finally, the use of MD has allowed us to know the extraction mechanism. The IL cation is positioned as the primary driver of physical extraction. When equilibrium is achieved, the cation is closer to the aromatic molecules than the anion. The diffusion coefficient plays a crucial role in extractive processes. Still, on this occasion, despite increasing considerably with temperature, it cannot overcome thermal agitation, and the equilibrium shifts to the left with increasing temperature. The MD is presented as a good tool for the qualitative analysis of each ionic liquid, as the results obtained are in line with the experimental ones. It should be noted that the compounds used in this work to synthesize the SC have been used as average representative compounds and that the composition of aromatics in lubricant bases is much more varied. The next step should be to experiment with factual lubricant bases. It is expected that the percentage of aromatics in the lubricant base will be below that set by law after a few extraction stages.

CRediT authorship contribution statement

Plácido Arenas-Fernández: Methodology, Validation, Investigation, Writing – original draft. **Inmaculada Suárez:** Conceptualization, Methodology, Formal analysis. **Baudilio Coto:** Conceptualization, Data curation, Software, Funding acquisition, Writing – original draft, Writing – review & editing.

Declaration of Competing Interest

The authors declare that they have no known competing financial interests or personal relationships that could have appeared to influence the work reported in this paper.

Data availability

No data was used for the research described in the article.

Appendix A. Supplementary material

Supplementary data to this article can be found online at https://doi.org/10.1016/j.seppur.2022.122160.

References

[1] F.M.T. Luna, A.N. Oliveira Filho, C.C.B. Araújo, D.C.S. Azevedo, C.L. Cavalcante, Adsorption of Polycyclic Aromatic Hydrocarbons from Heavy Naphthenic Oil Using Commercial Activated Carbons. 1. Fluid-Particle Studies, Ind. Eng. Chem. Res. 55 (29) (2016) 8176–8183.

[2] B. Coto, I. Suárez, M.J. Tenorio, I. Huerga, Extraction of aromatic and polyaromatic compounds with NMP: experimental and model description, Fluid Phase Equilib. 554 (2022), 113293, https://doi.org/10.1016/j.fluid.2021.113293.

[3] R. van Grieken, B. Coto, J.L. Peña, J.J. Espada, Application of a generalized model to the estimation of physical properties and description of the aromatic extraction from a highly paraffinic lubricating oil, Chem. Eng. Sci. 63 (2008) 711–720, https://doi.org/10.1016/j.ces.2007.10.013.

[4] B. Coto, R. van Grieken, J.L. Peña, J.J. Espada, A generalized model to predict the liquid-liquid equilibrium in the systems furfural + lubricating oils, Chem. Eng. Sci. 61 (2006) 8028–8039, https://doi.org/10.1016/j.ces.2006.09.037.

[5] B. Coto, I. Huerga, I. Suárez, V. Contreras, P. Pérez, Fast and simplified determination of PCA and aromatic carbon content of treated distilled aromatic extract (TDAE) by NMR, Anal. Bioanal. Chem. 414 (9) (2022) 3109–3119.

[6] M.A. Schwarz, A. Behnke, M. Brandt, A. Eisenträger, M. Hassauer, F. Kalberlah, A. Seidel, Semipolar polycyclic aromatic compounds: Identification of 15 priority substances and the need for regulatory steps under REACH regulation, Integr. Environ. Assess. Manag. 10 (2014) 415–428, https://doi.org/10.1002/ieam.1526.

[7] R. Van Grieken, B. Coto, E. Romero, J.J. Espada, Prediction of liquid-liquid equilibrium in the system furfural + heavy neutral distillate lubricating oil, Ind. Eng. Chem. Res. 44 (2005) 8106–8112, https://doi.org/10.1021/ie050069l.

[8] M.A. Mallah, L. Changxing, M.A. Mallah, S. Noreen, Y. Liu, M. Saeed, H. Xi, B. Ahmed, F. Feng, A.A. Mirjat, W. Wang, A. Jabar, M. Naveed, J.-H. Li, Q. Zhang, Polycyclic aromatic hydrocarbon and its effects on human health: An overeview, Chemosphere. 296 (2022) 133948, https://doi.org/10.1016/j.chemosphere.2022.133948.

[9] I. Burstyn, H. Kromhout, T. Partanen, O. Svane, S. Langård, W. Ahrens, T. Kauppinen, I. Stücker, J. Shaham, D. Heederik, G. Ferro, P. Heikkila, M. Hooiveld, C. Johansen, B.G. Randem, P. Boffetta, Polycyclic aromatic hydrocarbons and fatal ischemic heart disease, Epidemiology. 16 (2005) 744–750, https://doi.org/10.1097/01.ede.0000181310.65043.2f.

[10] R. Tong, X. Yang, H. Su, Y. Pan, Q. Zhang, J. Wang, M. Long, Levels, sources and probabilistic health risks of polycyclic aromatic hydrocarbons in the agricultural soils from sites neighboring suburban industries in Shanghai, Sci. Total Environ. 616–617 (2018) 1365–1373, https://doi.org/10.1016/j.scitotenv.2017.10.179.

[11] K. Kuklinska, L. Wolska, J. Namiesnik, Air quality policy in the U.S. and the EU - A review, Atmos. Pollut. Res. 6 (2015) 129–137, https://doi.org/10.5094/APR.2015.015.

[12] L.S. Maria-Elizabeth Gómez, N. Tapias, C. Vargas, J. Lizcano, PCA Reduction in Naphthenic Base Oils By HDT Conditions, Ciencia, Tecnol. y Futur. 4 (2010) 101–112.

[13] T. Luo, L. Zhang, C. Zhang, J. Ma, Z. Xu, X. Sun, S. Zhao, Role of water as the co-solvent in eco-friendly processing oil extraction: Optimization from experimental data and theoretical approaches, Chem. Eng. Sci. 183 (2018) 275–287, https://doi.org/10.1016/j.ces.2018.03.015.

[14] E. Von Lau, S. Gan, H.K. Ng, P.E. Poh, Extraction agents for the removal of polycyclic aromatic hydrocarbons (PAHs) from soil in soil washing technologies, Environ. Pollut. 184 (2014) 640–649, https://doi.org/10.1016/j.envpol.2013.09.010.

[15] Y. Tian, W.B. McGill, T.W. Whitcombe, J. Li, Ionic Liquid-Enhanced Solvent Extraction for Oil Recovery from Oily Sludge, Energy and Fuels. 33 (2019) 3429–3438, https://doi.org/10.1021/acs.energyfuels.9b00224.

[16] A. Arce, M.J. Earle, H. Rodríguez, K.R. Seddon, Separation of aromatic hydrocarbons from alkanes using the ionic liquid 1-ethyl-3-methylimidazolium bis ((trifluoromethyl) sulfonyl)amide, Green Chem. 9 (2007) 70–74, https://doi.org/10.1039/b610207g.

[17] P. Werner, S.; Haumann; M.; Wasserscheid, Ionic Liquids in Chemical Engineering, Chem. Eng. Process. Process Intensif. 1 (2010) 203–230.

[18] CHEMISTRY BASF'S SMART IONIC LIQUID, Chem. Eng. News Arch. 81 (2003) 9. https://doi.org/10.1021/cen-v081n013.p009.

[19] U. Domańska, A. Wiśniewska, Z. Dąbrowski, Liquid-liquid equilibrium studies on the removal of naphthalene / 2-methylnaphthalene / dibenzothiophene from model oil using ionic liquids, Fluid Phase Equilib. 556 (2022) 113397.

[20] P. Navarro, M. Larriba, N. Delgado-Mellado, M. Ayuso, M. Romero, J. García, F. Rodríguez, Experimental screening towards developing ionic liquid-based extractive distillation in the dearomatization of refinery streams, Sep. Purif. Technol. 201 (2018) 268–275, https://doi.org/10.1016/j.seppur.2018.03.024.

[21] G.W. Meindersma, A.R. Hansmeier, A.B. De Haan, Ionic liquids for aromatics extraction. Present status and future outlook, Ind. Eng. Chem. Res. 49 (2010) 7530–7540, https://doi.org/10.1021/ie100703p.

[22] R. Martnez-Palou, P. Flores, Perspectives of Ionic Liquids Applications for Clean Oilfield Technologies, Ion Liq. Theory, Prop. New Approaches. (2011), https://doi.org/10.5772/14529.

[23] K. Wendler, S. Zahn, F. Dommert, R. Berger, C. Holm, B. Kirchner, L. Delle Site, Locality and fluctuations: Trends in imidazolium-based ionic liquids and beyond, J. Chem. Theory Comput. 7 (2011) 3040–3044. https://doi.org/10.1021/ct200375v.

[24] C. Zhang, S.V. Malhotra, A.J. Francis, Toxicity of imidazolium- and pyridinium-based ionic liquids and the co-metabolic degradation of N-ethylpyridinium tetrafluoroborate, Chemosphere. 82 (2011) 1690–1695, https://doi.org/10.1016/j.chemosphere.2010.10.085.

[25] X. Chen, H. Sun, T. Zhang, H. Shang, Z. Han, Y. Li, Effects of pyridinium-based ionic liquids with different alkyl chain lengths on the growth of maize seedlings, J. Hazard. Mater. 427 (2022), 127868, https://doi.org/10.1016/j.jhazmat.2021.127868.

[26] R.P. Swatloski, J.D. Holbrey, R.D. Rogers, Ionic liquids are not always green: Hydrolysis of 1-butyl-3- methylimidazolium hexafluorophosphate, Green Chem. 5 (2003) 361–363, https://doi.org/10.1039/b304400a.

[27] A. Fernández, J.S. Torrecilla, J. García, F. Rodríguez, Thermophysical properties of 1-ethyl-3-methylimidazolium ethylsulfate and 1-butyl-3-methylimidazolium methylsulfate ionic liquids, J. Chem. Eng. Data. 52 (2007) 1979–1983, https://doi.org/10.1021/je7002786.

[28] J.D. Holbrey, W.M. Reichert, R.P. Swatloski, G.A. Broker, W.R. Pitner, K.R. Seddon, R.D. Rogers, Efficient, halide free synthesis of new, low cost ionic liquids: 1,3-dialkylimidazolium salts containing methyl- and ethyl-sulfate anions, Green Chem. 4 (2002) 407–413, https://doi.org/10.1039/b204469b.

[29] A.R. Ferreira, M.G. Freire, J.C. Ribeiro, F.M. Lopes, J.G. Crespo, J.A.P. Coutinho, An overview of the liquid-liquid equilibria of (ionic liquid + hydrocarbon) binary systems and their modeling by the conductor-like screening model for real solvents, Ind. Eng. Chem. Res. 50 (2011) 5279–5294, https://doi.org/10.1021/ie102471b.

[30] J. De Riva, V.R. Ferro, D. Moreno, I. Diaz, J. Palomar, Aspen Plus supported conceptual design of the aromatic-aliphatic separation from low aromatic content naphtha using 4-methyl-N-butylpyridinium tetrafluoroborate ionic liquid, Fuel Process. Technol. 146 (2016) 29–38, https://doi.org/10.1016/j.fuproc.2016.02.001.

[31] Y.J. Lin, N. Hossain, C.C. Chen, Modeling dissociation of ionic liquids with electrolyte NRTL model, J. Mol. Liq. 329 (2021), 115524, https://doi.org/10.1016/j.molliq.2021.115524.

[32] Z. Wang, W. Fan, D. Xu, S. He, H. Huang, J. Gao, Y. Wang, Liquid-Liquid-Phase Equilibrium for Quaternary Systems (n-Decane + 1-Tetradecene + 1-Methyl-naphthalene + Sulfolane/Dimethyl Sulfoxide) for Separation of 1-Methylnaph-thalene from FCC Diesel, J. Chem. Eng. Data. 66 (2021) 2803–2811, https://doi.org/10.1021/acs.jced.1c00194.

[33] N.D. F. G. Fonseca, A. Funke, Aspen plusTM modeling of fractional condensation schemes for production of fast pyrolysis bio-oil, 27th Eur. Biomass Conf. Exhib. (n. d.) 1227–1233. https://doi.org/10.5071/27thEUBCE2019-3BV.7.9.

[34] M.A. Usman, O.K. Fagoroye, T.O. Ajayi, A.J. Kehinde, ASPEN plus simulation of liquid–liquid equilibria data for the extraction of aromatics from waste tyre pyrolysis gasoline using organic and deep eutectic solvents: a comparative study, Appl. Petrochemical Res. 11 (2021) 113–122, https://doi.org/10.1007/s13203-020-00262-8.

[35] M. Han, S. Lin, M. Xu, Y. Jiang, Q. Yin, Y. Pang, Y. Song, Q. Li, Experiments and thermodynamic models for ternary liquid–liquid equilibrium systems of water + tetrahydrofurfuryl alcohol + solvents at different temperatures, J. Chem. Thermodyn. 167 (2022), https://doi.org/10.1016/j.jct.2021.106709.

[36] Z. Lei, C. Dai, X. Liu, L. Xiao, B. Chen, Extension of the UNIFAC model for ionic liquids, Ind. Eng. Chem. Res. 51 (2012) 12135–12144, https://doi.org/10.1021/ie301159v.

[37] Z. Rashid, C.D. Wilfred, N. Gnanasundaram, A. Arunagiri, T. Murugesan, Screening of ionic liquids as green oilfield solvents for the potential removal of asphaltene from simulated oil: COSMO-RS model approach, J. Mol. Liq. 255 (2018) 492–503, https://doi.org/10.1016/j.molliq.2018.01.023.

[38] U. Domańska, A. Pobudkowska, F. Eckert, Liquid–liquid equilibria in the binary systems (1,3-dimethylimidazolium, or 1-butyl-3-methylimidazolium methylsulfate + hydrocarbons), Green Chem. 8 (2006) 268–276, https://doi.org/10.1039/b514521j.

[39] S.T. Lin, S.I. Sandler, A priori phase equilibrium prediction from a segment contribution solvation model, Ind. Eng. Chem. Res. 41 (2002) 899–913, https://doi.org/10.1021/ie001047w.

[40] R. Xiong, S.I. Sandler, R.I. Burnett, An improvement to COSMO-SAC for predicting thermodynamic properties', Ind. Eng. Chem. Res. 53 (2014) 8936, https://doi.org/10.1021/ie501775s.

[41] Y.W. D. Xu, M. Zhang, J. Gao, L. Zhang, S. Zhou, Separation of heterocyclic nitro-gen compounds from coal tar fractions via ionic liquids: COSMO-SAC screening and experimental study, Chem. Eng. Sci. 206 (2019) 1199–1217. https://doi.org/https://doi.org/ 10.1080/00986445.2018.1552855.

[42] Z. Zhu, H. Li, Y. Xu, W. Zhang, Y. Shen, J. Gao, L. Wang, Y. Wang, Quantum chemical calculation, molecular dynamics simulation and process design for separation of heptane - butanol using ionic liquids extraction, J. Mol. Liq. 316 (2020), 113851, https://doi.org/10.1016/j.molliq.2020.113851.

[43] W. Zhang, Z. Chen, Y. Shen, G. Li, Y. Dai, J. Qi, Y. Ma, S. Yang, Y. Wang, Molecular Mechanism and Extraction Performance Evaluation for Separation of Methanol and n-Hexane via Ionic Liquids as Extractant, ACS Sustain. Chem. Eng. 8 (2020) 8700–8712, https://doi.org/10.1021/acssuschemeng.0c02234.

[44] H. Li, G. Sun, D. Li, L. Xi, P. Zhou, X. Li, J. Zhang, X. Gao, Molecular interaction mechanism in the separation of a binary azeotropic system by extractive distillation with ionic liquid, Green, Energy Environ. 6 (2021) 329–338, https://doi.org/10.1016/j.gee.2020.11.025.

[45] S.V. Lyulin, A.D. Glova, S.G. Falkovich, V.A. Ivanov, V.M. Nazarychev, A.V. Lyulin, S.V. Larin, S.V. Antonov, P. Ganan, J.M. Kenny, Computer Simulation of Asphaltenes 1, Pet. Chem. 58 (12) (2018) 983–1004.

[46] J.N. Canongia Lopes, J. Deschamps, A.A.H. Pádua, Modeling Ionic Liquids Using a Systematic All-Atom Force Field, J. Phys. Chem. B. 108 (6) (2004) 2038–2047.

[47] F. Dommert, K. Wendler, R. Berger, L. Delle Site, C. Holm, Force Fields for Studying the Structure and Dynamics of Ionic Liquids: A Critical Review of Recent Developments, ChemPhysChem 13 (7) (2012) 1625–1637.

[48] D. Bedrov, J.-P. Piquemal, O. Borodin, A.D. MacKerell, B. Roux, C. Schröder, Molecular Dynamics Simulations of Ionic Liquids and Electrolytes Using Polarizable Force Fields, Chem. Rev. 119 (13) (2019) 7940–7995.

[49] P. Nancarrow, N. Mustafa, A. Shahid, V. Varughese, U. Zaffar, R. Ahmed, N. Akther, H. Ahmed, I. Alzubaidy, S. Hasan, Y. Elsayed, Z. Sara, Technical Evaluation of Ionic Liquid-Extractive Processing of Ultra Low Sulfur Diesel Fuel, Ind. Eng. Chem. Res. 54 (2015) 10843–10853, https://doi.org/10.1021/acs.iecr.5b02825.

[50] B.S. Lee, S.T. Lin, Prediction of phase behaviors of ionic liquids over a wide range of conditions, Fluid Phase Equilib. 356 (2013) 309–320, https://doi.org/10.1016/j.fluid.2013.07.046.

[51] M. Diedenhofen, A. Klamt, COSMO-RS as a tool for property prediction of IL mixtures-A review, Fluid Phase Equilib. 294 (2010) 31–38, https://doi.org/10.1016/j.fluid.2010.02.002.

[52] Z. Lei, J. Zhang, Q. Li, B. Chen, UNIFAC model for ionic liquids, Ind. Eng. Chem. Res. 48 (2009) 2697–2704, https://doi.org/10.1021/ie801496e.

[53] H. Berendsen, D. Vanderspoel, R. Vandrunen, GROMACS: a messagepassing parallel molecular dynamics implementation, Comput. Phys. Commun. 91 (1995) 43–56.

[54] T. Köddermann, D. Paschek, R. Ludwig, Molecular dynamic simulations of ionic liquids: A reliable description of structure, thermodynamics and dynamics, ChemPhysChem. 8 (2007) 2464–2470, https://doi.org/10.1002/cphc.200700552.

[55] L. Zhang, M.L. Greenfield, Effects of Polymer Modification on Properties and Microstructure of Model Asphalt Systems, Energy and Fuels. 22 (5) (2008) 3363–3375.

[56] K. Sonibare, L. Rathnayaka, L. Zhang, Comparison of CHARMM and OPLS-aa forcefield predictions for components in one model asphalt mixture, Constr. Build. Mater. 236 (2020), 117577, https://doi.org/10.1016/j.conbuildmat.2019.117577.

[57] P. Arenas, I. Suárez, B. Coto, Combination of molecular dynamics simulation, COSMO-RS, and experimental study to understand extraction of naphthenic acid, Sep. Purif. Technol. 280 (2022) 119810.

[58] L. Petridis, J.C. Smith, A Molecular Mechanics Force Field for Lignin, J. Comput. Chem. (2008), https://doi.org/10.1002/jcc.

[59] W.G. Hoover, Canonical dynamics: Equilibrium phase-space distributions, Phys. Rev. A. 31 (3) (1985) 1695–1697.

[60] A. Parrinello, M. and Rahman, Polymorphic Transitions in Single Crystals: A New Molecular Dynamics Method, J. Appl. Phys. 52 (1981) 7182–7190. https://doi.org/10.1063/1.328693.

[61] G.S. Anderson, R.C. Miller, A.R.H. Goodwin, Static dielectric constants for liquid water from 300 K to 350 K at pressures to 13 MPa using a new radiofrequency resonator, J. Chem. Eng. Data. 45 (4) (2000) 549–554.

[62] B. Coto, I. Suárez, M.J. Tenorio, S. Nieto, N. Alvarez, J.L. Peña, Oil acidity reduction by extraction with imidazolium ionic liquids: Experimental, COSMO description and reutilization study, Sep. Purif. Technol. 254 (2021), 117529, https://doi.org/10.1016/j.seppur.2020.117529.

[63] T.G.A. Youngs, C. Hardacre, Application of static charge transfer within an ionic-liquid force field and its effect on structure and dynamics, ChemPhysChem. 9 (2008) 1548–1558, https://doi.org/10.1002/cphc.200800200.

[64] M.R. Islam, Y. Hao, M. Wang, C.C. Chen, Prediction of Asphaltene Precipitation in Organic Solvents via COSMO-SAC, Energy and Fuels. 31 (2017) 8985–8996, https://doi.org/10.1021/acs.energyfuels.7b01129.

[65] H. Tokuda, K. Hayamizu, K. Ishii, M.A.B.H. Susan, M. Watanabe, Physicochemical properties and structures of room temperature ionic liquids. 1. Variation of anionic species, J. Phys. Chem. B. 108 (2004) 16593–16600, https://doi.org/10.1021/jp047480r.

[66] O. Borodin, Polarizable force field development and molecular dynamics simulations of ionic liquids, J. Phys. Chem. B. 113 (2009) 11463–11478, https://doi.org/10.1021/jp905220k.